

Illusion optics

Yun LAI (赖耘), Jack NG (吴紫辉), Huan-yang CHEN (陈焕阳), Zhao-qing ZHANG (张昭庆),
C. T. CHAN (陈子亭)[†]

*Department of Physics, Hong Kong University of Science and Technology, Clear Water Bay, Kowloon, Hong Kong, China
E-mail: phchan@ust.hk*

Received March 10, 2010; accepted March 20, 2010

The technique of “transformation optics” establishes a correspondence between coordinate transformation and material constitutive parameters. Most of the transformation optics mappings give metamaterials that have graded positive refractive indices that can steer light in curves defined by the coordinate transformation. We will focus on those “folded-geometry mappings” that give negative refractive index materials that have special wave scattering properties. One interesting example is a kind of remote illusion device that can transform the stereoscopic image of an object into the illusion of some other object of our choice. The conceptual device can create the illusion without touching or encircling the object. For any incident wave, the device transforms the scattered waves of the original object into that of the object chosen for illusion outside a virtual boundary. We will illustrate some possible applications of this type of metamaterial remote device, including “cloaking at a distance,” partial cloaking, cloaking from an embedded device, revealing a hidden object inside a container, turning the image of one object into that of another object, and seeing through a wall. The feasibility of building this remote illusion device by metamaterials will also be discussed.

Keywords metamaterial, transformation optics, transformation media, cloaking, illusion, camouflage

PACS numbers 41.20.Jb, 42.79.-e

Contents

1	Introduction	308
2	Theory	310
2.1	Transformation optics	310
2.2	Illusion optics	310
3	Cloaking effects by using illusion devices designed in cylindrical geometry	311
3.1	Cloaking at a distance	311
3.2	Partial cloaking	313
3.3	Cloaking from an embedded device	313
3.4	Revealing a hidden object inside a container	314
4	Cloaking and illusion effects by using illusion devices designed in Cartesian geometry	315
4.1	Transforming the stereoscopic image of a dielectric spoon into that of a metallic cup	315
4.2	Seeing through a wall	315
5	Conclusions and discussion	316
	Acknowledgements	317
	References	317

1 Introduction

As the saying goes, “seeing is believing.” Throughout

history, witnessing with the eyes has been used as proof of existence or as evidence. On the other hand, the effects of illusions, such as mirages, have been well known to lead people to draw incorrect conclusions, sometimes with dire consequences. Illusion effects have fascinated people for centuries and have inspired myths, novels, and films.

One of the most fascinating illusion effects is invisibility cloaking. Recently, cloaking has experienced rapid development in both theory and experiment [1–32]. One big advance is a new theory called transformation optics that can steer light along arbitrary curves and thus provides a theoretical foundation for cloaking [1–4]. In transformation optics, when a coordinate transformation has been applied to Maxwell’s equations, a spatially distributed set of constitutive parameters is obtained, which guarantees a mapping relation between the electromagnetic states in the original space and the new states in the transformed space. Transformation optics has many novel applications [1–19, 28, 33–50]. In the case of cloaking, a cloaking shell that functions as a sphere of free space is formed by a coordinate transformation from the sphere to the shell. When a beam of light enters the shell, it is bended around the interior region and then

directed to come out on the other side of the shell in a way as if it has passed through a region of free space. In the process, light is prevented from entering the interior region as well as being scattered by the hidden object inside. Invisibility is thus achieved.

It is not easy to build such a cloaking shell. This is because that the constitutive parameters of the shell, which is obtained from transformation optics, have graded and anisotropic indexes, and tend to extreme values at the interior boundary of the shell. Fortunately, these parameters are enabled by a new kind of man-made materials called metamaterials [51–56], which are made of carefully designed subwavelength structures. They can be engineered to offer electromagnetic properties that are difficult or impossible to achieve with conventional materials, such as artificial magnetism [51] or negative refractive index materials [52–56]. The first experimental realization of cloaking was carried out at microwave frequencies by using metamaterials composed of split-ring resonators [12]. Subsequently, an optical version of the cloak has been proposed based on metal wire metamaterials [13]. Recently, there are also some approaches using nonresonant structures due to their low-loss and broadband feature in optical regime. A non-Euclidean cloak has been proposed using transformation optics in Non-Euclidean space and thus contains no extreme constitutive parameters [14]. Another approach is a so-called “carpet cloak,” which also avoids extreme parameters by making a cloak attached to a ground plane [15]. The “carpet cloak” has been experimentally demonstrated at microwaves and near infrared frequencies by using dielectrics structures [16–18]. Waveguides of varying height have also been utilized to make invisibility cloaks [19].

Besides the light-bending transformation optics approach, there exist other ways to realize cloaking [20–32]. Even before transformation optics, it has been proposed that by making a plasmonic coating on a particle, the scattering cross section of the particle can be reduced dramatically [20], achieving a cloaking effect. The principle of this cloaking effect is the “cancellation” of the particle and its plasmonic coatings, and this approach exhibits a possibility of achieving multifrequency functionality as well as “cloaking a sensor” [20–22]. Another interesting finding is the possibility of cloaking outside a cloaking shell [25–27]. It was first mathematically shown that in the quasistatic limit, a finite collection of polarizable line dipoles or quadrupoles can be cloaked within a distance from a coated cylinder with a shell permittivity of $\varepsilon_s \approx -\varepsilon_m \approx -\varepsilon_c$, where ε_m is the matrix permittivity, and ε_c is the core permittivity [25]. This cloaking effect is induced by the anomalous localized resonances on the surface of the negative permittivity shell that almost “cancels” the incident field acting on the dipole/quadrupole. However, it has been pointed out that this cloaking effect fails for large-sized objects [27].

Recently, we have proposed another scheme to realize “cloaking at a distance” using transformation optics [28]. In theory, our approach works for any objects of any material makeup and any shape at a particular frequency. The key concept behind our idea is “complementary medium”, which is a special form of negative refraction index material formed by applying “folded-geometry mappings” (see, e.g., Ref. [5]) in transformation optics. The concept of complementary media was first proposed to explain the imaging effect of devices, such as the “perfect lens” [57–59]. It is known that complementary medium has a special property of optically “cancelling” a certain volume of space at its working frequency. Based on this, we proposed to cloak an object in two steps. First, the object as well as its surrounding space is “canceled” by using a complementary medium layer with an embedded complementary “image” of the object. Then, the “canceled” space is “refilled” by using a “restoring medium,” which restores the correct optical path that light should have experienced passing through a region of free space. The combination of the complementary medium and restoring medium constitutes our cloaking device. In this approach, cloaking is realized by the multiple scattering processes between the object and its cloaking device. For any incident waves, the scattering pattern of both object and the cloaking device are changed in an amazing way such that the total scattered waves outside a virtual boundary almost vanish. This mechanism is very different from that of previous light-bending approaches. As a result, our cloaking device can realize “cloaking at a distance” for any incident waves.

There are some interesting applications that arise from the “remote” nature of our cloaking device. One is the realization of “partial cloaking,” i.e., making part of an object invisible while retaining the other parts unchanged. This further enables “seeing through the wall” by making a virtual hole on a wall and “revealing a hidden object inside a container” by making the container invisible without cloaking objects inside. “Cloaking from an embedded device” also becomes possible, in contrast to previous cloaking devices that must enclose objects from outside.

Most recently, another innovative way of cloaking utilizing active sources instead of passive metamaterials has been proposed [29–32]. The advantage of active sources is that the functionality of device can be made into broadband in theory, in contrast to those of resonant metamaterials. It was shown that external cloaking can also be achieved by using several points/disks of active multipole sources [30]. Recently, we have extended the scheme to simple sources on continuous curves and to create arbitrary illusions [32].

Since invisibility can be viewed as an illusion of free space, cloaking is actually a special case of the illusion tricks. Similar to the concept of cloaking, turning an

object into a stereoscopic illusion has a long history of public fantasy. One famous example is the 72 transformation magic of the Monkey King in *Pilgrimage to the West* in the Chinese literature. Recently, we show that the cloaking device can be modified to become an illusion device [33], i.e., a device that changes the appearance of an object into that of another object of our choice. The recipe is to change the “restoring medium” such that the object for illusion is restored instead of simply free space. The scattered waves of the whole system outside a virtual boundary will be changed into those of the object for illusion under the same incident waves, thus any observer outside will see the stereoscopic illusion instead of the original object. This simple idea proves, in a scientific way, an exciting fact that a total illusion effect for all angles is possible (unlike the mirror, TV, or mirage that work only for certain angle of view at certain distances).

It should be mentioned that before the idea of illusion optics was proposed, some specific illusion effects have already been discussed, such as the “cylindrical superlens” [34] that behaves in a similar way of “superlens” [57], the shifted-position illusion in a similar shell structure [35], the “superscatterer” that appears like a scatterer much bigger than the device [36], “concealing an entrance” by using a rectangular superscatterer [37], the “reshaper” that is an illusion of PEC with arbitrary shape [38], the “superabsorber” that is an illusion of a bigger absorber [39], etc. Our work actually gives a systematic understanding and unified theory for these illusion effects. Other interesting ideas that appear at about or after our work are “a tunable electromagnetic gateway” [40], an “illusion media” cloak that turns the original light-bending cloaks into its illusion counterparts [41], a “moving particle” illusion realized by positive parameter metamaterials [42]. Most of the efforts mentioned above are theoretical. The lack of experimental work is probably due to current difficulties of making metamaterials of the precise permeability and permittivity at precise positions and especially metamaterials with negative parameters. This will be discussed in detail later.

In Section 2, we first give a brief introduction to the theory of transformation optics. Then, we prove our scheme of the external cloaking and illusion effects by using the folded-geometry mapping in transformation optics. In Section 3, we demonstrate some cloaking effects by using illusion devices designed in the cylindrical geometry, including cloaking at a distance, partial cloaking, cloaking from an embedded device, and revealing a hidden object inside a container. In Section 4, we show illusions and cloaking effects realized by using illusion devices designed in Cartesian geometry, including turning the stereoscopic image of a spoon into that of a cup and seeing through the wall by opening a virtual hole. In Section 5, the conclusion is made, and the feasibility

of making cloaking and illusion devices is discussed.

2 Theory

2.1 Transformation optics

We start from the Maxwell’s equations

$$\nabla \times \mathbf{E} + i\omega\boldsymbol{\mu}\mathbf{H} = 0, \quad \nabla \times \mathbf{H} - i\omega\boldsymbol{\varepsilon}\mathbf{E} = 0 \quad (1)$$

The central idea of transformation optics is that when a coordinate mapping $\mathbf{x}' = \mathbf{x}'(\mathbf{x})$ is applied, the Maxwell’s equation in the new coordinate can be written as:

$$\nabla \times \mathbf{E}' + i\omega\boldsymbol{\mu}'\mathbf{H}' = 0, \quad \nabla \times \mathbf{H}' - i\omega\boldsymbol{\varepsilon}'\mathbf{E}' = 0 \quad (2)$$

where $\boldsymbol{\varepsilon}$ and $\boldsymbol{\mu}$ are permittivity and permeability in the original space \mathbf{x} , $\boldsymbol{\varepsilon}'$ and $\boldsymbol{\mu}'$ are permittivity and permeability in the new space \mathbf{x}' , i.e., the transformation medium. This means that the form of Maxwell’s equations is preserved after a coordinate transformation. Therefore, the coordinate transformation guarantees a mapping relationship between the electromagnetic states in the original space and the new states in the transformed space. The electromagnetic fields in the transformation medium can be explicitly written as:

$$\mathbf{E}'(\mathbf{x}') = (\mathbf{A}^T)^{-1}\mathbf{E}(\mathbf{x}), \quad \mathbf{H}'(\mathbf{x}') = (\mathbf{A}^T)^{-1}\mathbf{H}(\mathbf{x}) \quad (3)$$

where $\mathbf{A} = (\nabla\mathbf{x}')^T$ with components $A_{ij} = \partial x'_i/\partial x_j$. The permittivity and permeability of the transformation medium can be written as:

$$\begin{aligned} \boldsymbol{\varepsilon}'(\mathbf{x}') &= \mathbf{A}\boldsymbol{\varepsilon}(\mathbf{x})\mathbf{A}^T/\det \mathbf{A} \\ \boldsymbol{\mu}'(\mathbf{x}') &= \mathbf{A}\boldsymbol{\mu}(\mathbf{x})\mathbf{A}^T/\det \mathbf{A} \end{aligned} \quad (4)$$

The detailed proof of the invariance of the form of Maxwell’s equations can be found in Ref. [4]. When the coordinate mapping $\mathbf{x}' = \mathbf{x}'(\mathbf{x})$ is determined, the transformation medium is also determined.

2.2 Illusion optics

We shall prove here that by using the complementary medium and the restoring medium designed from transformation optics, we are able to transform an object into an illusion of another object of our choice. In order to prove this, we consider two worlds, one is the real world with the original object and the illusion device, and the other is the illusion world with only the object for illusion. In order to achieve a total illusion effect for all angles, the far field electromagnetic responses of the original object plus the illusion device must be equal to the illusion object, for any incident waves.

Consider the configuration depicted in Fig. 1. In Fig. 1(a), an illusion device is placed next to a domain that contains a man (the object). The passive device causes any observer outside the virtual boundary (the dashed curves) to see the image of a woman [the illusion, Fig.

1(b)] instead. In other words, such an illusion device makes the electromagnetic fields outside the virtual boundary in both the real [Fig. 1(a)] and illusion [Fig. 1(b)] worlds the same, irrespective of the profile and direction of the incident waves. A schematic blueprint for the device is shown in Fig. 1(c). The device itself can be divided into two regions, i.e., regions 1 and 2. Region 2 includes the complementary medium used to annihilate the optical signature of the man, while region 1 includes the restoring medium that creates the image of the woman. Both media are designed using transformation optics. The complementary medium is formed by a coordinate transformation of folding region 3, which contains the man, into region 2. The restoring medium is formed by a coordinate transformation of compressing region 4 in Fig. 1(d), which contains the illusion, into region 1. The permittivity and permeability tensors of both media in the illusion device are obtained by $\epsilon^{(2)} = \mathbf{A}\epsilon^{(3)}\mathbf{A}^T/\det\mathbf{A}$, $\mu^{(2)} = \mathbf{A}\mu^{(3)}\mathbf{A}^T/\det\mathbf{A}$, $\epsilon^{(1)} = \mathbf{B}\epsilon^{(4)}\mathbf{B}^T/\det\mathbf{B}$ and $\mu^{(1)} = \mathbf{B}\mu^{(4)}\mathbf{B}^T/\det\mathbf{B}$, where $\epsilon^{(i)}$ and $\mu^{(i)}$ are the permittivity and permeability tensors in region i , respectively. \mathbf{A} and \mathbf{B} are the Jacobian transformation tensors with components $A_{ij} = \partial x_i^{(2)}/\partial x_j^{(3)}$ and $B_{ij} = \partial x_i^{(1)}/\partial x_j^{(4)}$, corresponding to the coordinate transformations of folding region 3 into region 2 and compressing region 4 into region 1, respectively.

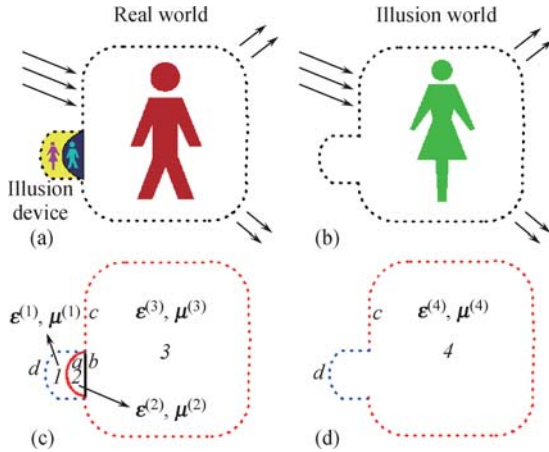


Fig. 1 The working principle of an illusion device that transforms the stereoscopic image of the object (say a man) into that of the illusion (say a woman). (a) The object and the illusion device in real world. (b) The object and the illusion device in illusion world. (c) The physical description of the illusion device. It is composed of the complementary medium (region 2) that optically “cancels” a piece of space including the man (region 3), and the restoring medium (region 1) that restores a piece of the illusion space including the illusion [region 4 in (d)].

The electromagnetic fields in the complementary and the restoring media can also be obtained from transformation optics as $\mathbf{E}^{(2)} = (\mathbf{A}^T)^{-1}\mathbf{E}^{(3)}$, $\mathbf{H}^{(2)} = (\mathbf{A}^T)^{-1}\mathbf{H}^{(3)}$, $\mathbf{E}^{(1)} = (\mathbf{B}^T)^{-1}\mathbf{E}^{(4)}$, and $\mathbf{H}^{(1)} = (\mathbf{B}^T)^{-1}\mathbf{H}^{(4)}$, where $\mathbf{E}^{(i)}$ and $\mathbf{H}^{(i)}$ are the electric and magnetic fields in region i , respectively. From the match-

ing of the boundary conditions on surface a (the red solid curve) between the complementary medium and the restoring medium, we have $\mathbf{E}_t^{(2)}(a) = \mathbf{E}_t^{(1)}(a)$ and $\mathbf{H}_t^{(2)}(a) = \mathbf{H}_t^{(1)}(a)$, where subscript t indicates transverse components along the surface. Both the folding transformation, \mathbf{A} , and compression transformation, \mathbf{B} , map one part of the virtual boundary, i.e., surface c (the red dashed curves), to surface a . If this one-to-one mapping from c to a is the same for both \mathbf{A} and \mathbf{B} , i.e., $\mathbf{x}_a^{(2)}(\mathbf{x}_c^{(3)}) = \mathbf{x}_a^{(1)}(\mathbf{x}_c^{(4)})$, then we can obtain that $\mathbf{E}_t^{(3)}(c) = \mathbf{E}_t^{(4)}(c)$ and $\mathbf{H}_t^{(3)}(c) = \mathbf{H}_t^{(4)}(c)$ on surface c from transformation optics in curved coordinates. In addition, we also have $\mathbf{E}_t^{(1)}(d) = \mathbf{E}_t^{(4)}(d)$ and $\mathbf{H}_t^{(1)}(d) = \mathbf{H}_t^{(4)}(d)$ on surface d (the blue dashed curves), as long as d is mapped to itself during transformation \mathbf{B} . Therefore, the tangential components of the electromagnetic fields on the whole virtual boundary (c and d) are exactly the same in the real and illusion worlds, and consequently, by the uniqueness theorem, the electromagnetic fields outside are also the same. Any observer outside the virtual boundary will see electromagnetic waves as if they were scattered from the illusion object (the woman and nothing else). More details can be found in the Auxiliary Material of Ref. [33].

For the special case of cloaking, the object in illusion world in Fig. 1 should be replaced with empty space left in region 4 [Fig. 1(d)], where the restoring medium (region 1) is transformed from. In this way, the illusion device is turned into a cloaking device that works in a remote way.

It should be mentioned that the illusion device may not necessarily have an overlapping with the virtual boundary, i.e., surface d . For the case of no overlapping, the restoring medium becomes a core medium surrounded by a layer of the complementary medium. The illusion effects will be the same. In the following section, we show some applications of illusion devices designed in cylindrical geometry, including cloaking at a distance, partial cloaking, cloaking from an embedded device, and revealing a hidden object inside a container. All the numerical simulations below are demonstrated using a finite element solver (Comsol Multiphysics) and are in two dimensions. In two dimensions, the electromagnetic waves can be decoupled into TE waves (E along the z direction) and TM waves (H along the z direction). We show only the TE results for brevity and the parameters can be tuned to work for both TE and TM waves.

3 Cloaking effects by using illusion devices designed in cylindrical geometry

3.1 Cloaking at a distance

First, we show a scheme of folded-geometry mapping in

Fig. 1(a), a circular layer of complementary media with parameters $\boldsymbol{\varepsilon}'$ and $\boldsymbol{\mu}'$ that optically cancel an outer circular layer of air. The complementary medium can be obtained by folding a layer of air ($b < r < c$) back into the layer of complementary medium ($a < r' < b$). Consider a general coordinate transformation of the form $r = f(r')$ [28], in which $f(r')$ is a continuous function of r' that satisfies $f(b) = b$ and $f(a) = c$.

Then, $\boldsymbol{\varepsilon}'$ and $\boldsymbol{\mu}'$ of the complementary medium can be obtained from Eq. (4) and written as:

$$\begin{aligned}\varepsilon'_r &= \mu'_r = f(r')/r' f'(r'), \\ \varepsilon'_\theta &= \mu'_\theta = r' f'(r')/f(r'), \\ \varepsilon'_z &= \mu'_z = f(r')f'(r')/r'.\end{aligned}\quad (5)$$

For $f(r') = (r' - b) \cdot (c - b)/(a - b) + b$, which is a simple linear mapping, $\boldsymbol{\varepsilon}'$ and $\boldsymbol{\mu}'$ are anisotropic. However, if we choose $f(r') = b^2/r'$ and $c = b^2/a$, we can obtain isotropic parameters $\boldsymbol{\varepsilon}'$ and $\boldsymbol{\mu}'$ as $\mu'_r = \mu'_\theta = -1$, $\varepsilon'_z = -b^4/r'^4$ for TE waves, and $\varepsilon'_r = \varepsilon'_\theta = -1$, $\mu'_z = -b^4/r'^4$ for TM waves.

In order to restore the optical path, we use a restoring medium (core material) with $\mu''_r = \mu''_\theta = \varepsilon''_z \cdot a^2/c^2 = 1$ for TE waves and $\varepsilon''_r = \varepsilon''_\theta = \mu''_z \cdot a^2/c^2 = 1$ for TM waves, which are obtained by coordinate transformation of $r = c/a \cdot r''$, i.e., by compressing a large circle of air with radius c into a small circle with radius a . With such a core material, the wave experiences the same optical path as that in a circle of air with a radius c . In this way, the whole system, including the outer air layer, the complementary medium layer, and the core material, is optically equal to a circle of air with radius c , and it is thus invisible to any form of external illumination.

Now, suppose that an object of permittivity ε_o and permeability $\boldsymbol{\mu}_o$ is added in the outer circular layer of air, and we want to make it invisible. It is always possible to include a complementary “image” of the object with parameters $\boldsymbol{\varepsilon}'_o$ and $\boldsymbol{\mu}'_o$ as:

$$\begin{aligned}\frac{\varepsilon'_{or}}{\varepsilon_{or}} &= \frac{\mu'_{or}}{\mu_{or}} = \frac{f(r')}{r'} \frac{1}{f'(r')} \\ \frac{\varepsilon'_{o\theta}}{\varepsilon_{o\theta}} &= \frac{\mu'_{o\theta}}{\mu_{o\theta}} = \frac{r'}{f(r')} f'(r') \\ \frac{\varepsilon'_{oz}}{\varepsilon_{oz}} &= \frac{\mu'_{oz}}{\mu_{oz}} = \frac{f(r')}{r'} f'(r')\end{aligned}\quad (6)$$

in the complementary media layer, as shown in Fig. 1(b). In this way, the object of ε_o and $\boldsymbol{\mu}_o$ is optically “canceled”. This recipe suggests a way to conceal an object from electromagnetic waves within a specific distance outside the cloak, i.e., cloaking at a distance.

In the following, we carry out full wave simulations using the finite-element software “Comsol Multiphysics” to demonstrate “cloaking at a distance”. We consider a TE incident plane wave from below or a point source with wavelength $\lambda = 1$ unit. In Fig. 3(a), we first

demonstrate the scheme shown in Fig. 2(a), i.e., a shell of complementary medium ($0.5 < r' < 1$) and a core of restoring medium ($r'' < 0.5$) that should be invisible. A linear transformation mapping $f(r') = 3 - 2r'$ is applied. Moreover, we obtain the following parameters for the complementary medium and the core medium: $\mu'_r = (r' - 1.5)/r'$, $\mu'_\theta = r'/(r' - 1.5)$, $\varepsilon'_z = (4r' - 6)/r'$, and $\varepsilon''_z = 16$. The absence of scattered waves in Fig. 3(a) clearly verifies the invisibility of the whole system. Next, we demonstrate cloaking at a distance by using the scheme shown in Fig. 2(b). The object to be cloaked is chosen to be a dielectric curved sheet of thickness 0.3 with parameters $\varepsilon_o = 2$ and $\mu_o = 1$, positioned between the circles of $r = 1.5$ and $r = 1.8$. In Fig. 3(b), the scattering pattern of such a single dielectric curved sheet is shown. In order to make the object invisible, we modify the complementary medium layer in Fig. 3(a) to include a complementary “image” of the curved sheet with parameters $\varepsilon'_{oz} = 2\varepsilon'_z$ and $\boldsymbol{\mu}'_o = \boldsymbol{\mu}'$, positioned between the circles of $r' = 0.6$ and $r' = 0.75$. In Fig. 3(c), we clearly show that the total scattered electric fields of the illusion device and the curved sheet are almost zero, which indicates a good cloaking effect. In particular, we note that the invisibility cloak does not cover the object here. The cloaking effect comes from the multiple scattering between the illusion device and the object, which induces some high-intensity evanescent waves on the surface of the illusion device. We note that there is no constraint on the shape or size of the object to be cloaked, as long as it fits into the region bounded between $b < r < c$. In Fig. 3(d), we demonstrate the cloaking of two curved sheets. The sheet on the left bounded between $1.2 < r < 1.5$ has an anisotropic permeability of $\mu_{or} = 1$ and $\mu_{o\theta} = -1$. The sheet on the downside bounded between $1.5 < r < 1.8$ has a linearly changing permittivity of $\varepsilon_o = 1 + (1.8 - r)/0.3$. In this case, two complementary “images” are embedded at the corresponding imaging positions in the negative index shell. One “image” is of $\mu'_{or} = \mu'_r$, $\mu'_{o\theta} = -\mu'_\theta$, and $\varepsilon'_{oz} = \varepsilon'_z$, and the other “image” is of $\varepsilon'_{oz} = \varepsilon'_z [1 - (0.6 - r')/0.15]$ and $\boldsymbol{\mu}'_o = \boldsymbol{\mu}'$. A perfect cloaking effect is demonstrated

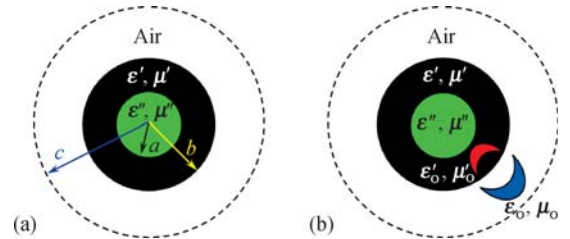


Fig. 2 The scheme of cloaking at a distance. (a) An invisible device composed of a shell of complementary median of $\boldsymbol{\varepsilon}'$, $\boldsymbol{\mu}'$ ($a < r' < b$) formed by folding the shell of $b < r < c$ into $a < r' < b$, and a restoring core material of $\boldsymbol{\varepsilon}'$, $\boldsymbol{\mu}''$ ($r'' < a$). (b) A scheme to cloak an object of ε_o , $\boldsymbol{\mu}_o$ by placing a complementary “image” of the object $\boldsymbol{\varepsilon}'_o$, $\boldsymbol{\mu}'_o$ in the complementary media layer of the device shown in (a).

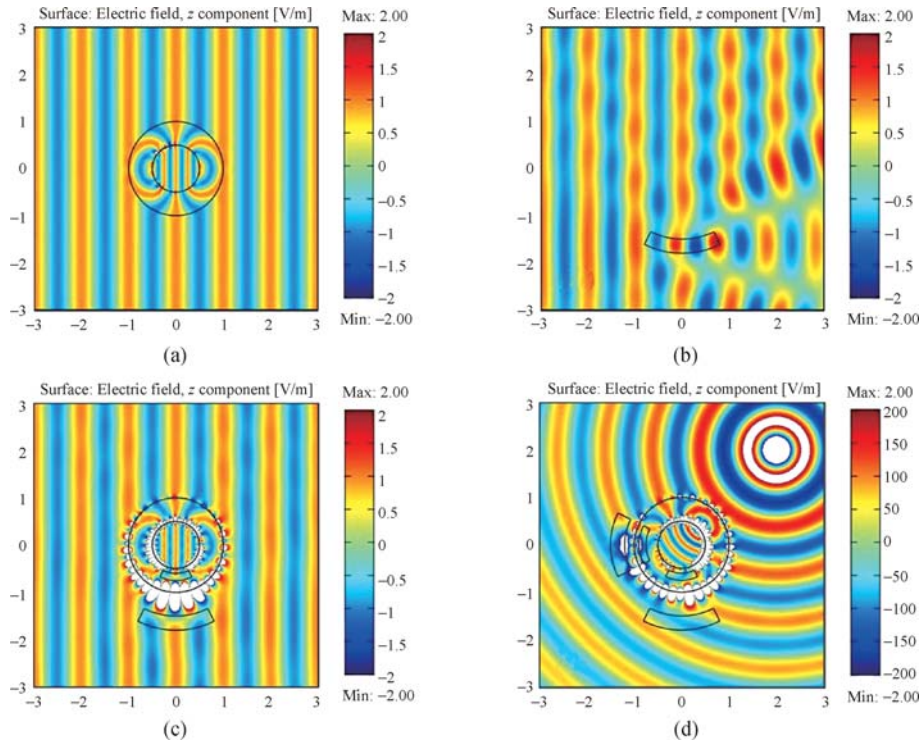


Fig. 3 Snapshots of the total electric fields under an incident TE plane wave from below [(a)–(c)] and a point source (d). (a) The demonstration of Fig. 2(a). Invisibility is achieved by the combination of a shell of complementary medium ($0.5 < r' < 1$) and a core of restoring medium ($r'' < 0.5$). (b) Scattering of a curved sheet of thickness 0.3, with permittivity $\epsilon_o = 2$. (c) The curved sheet in (b) is cloaked by embedding a complementary “image” of the sheet in the complementary medium layer of the device in (a). (d) Two curved sheets, one on the left has anisotropic permeability $\mu_{or} = 1$ and $\mu_{o\theta} = -1$ and the other has permittivity $\epsilon_o = 1 + (1.8 - r)/0.3$, are both cloaked by an invisibility cloak designed accordingly.

with a point source positioned at (2, 2).

3.2 Partial cloaking

By using the “remote” property of the illusion device, we demonstrate a partial cloaking effect, in which only a part of an object is “cloaked,” while the other parts remain unaffected. In Fig. 4(a), we show that the scattering of a thick curved sheet bounded between $1.2 < r < 1.8$ is changed by an illusion device that “cloaks” the inner part of the sheet, i.e., $1.2 < r < 1.5$, rendering the scattering pattern to become almost the same as that of a thin curved sheet of $1.5 < r < 1.8$, as shown in Fig. 4(b). This means that the thick sheet is partially cloaked

and therefore is optically turned into a thin sheet. Here, a linear transformation mapping $f(r') = 2 - r'$ is applied to obtain the parameters of the complementary medium layer of $0.5 < r' < 1$. The restoring core is of $\epsilon''_z = 9$. The total effect is that the cloaking effect is limited within a virtual boundary of $r = 1.5$.

3.3 Cloaking from an embedded device

The cloaking devices proposed previously require the cloaking shell to enclose the object. Here, we illustrate that our cloaking scheme allows us to cloak from within the object. We will cloak a dielectric shell of $\epsilon_o = 2$ and $\mu_o = 1$ bounded between $1.5 < r < 1.8$, as shown in Fig.

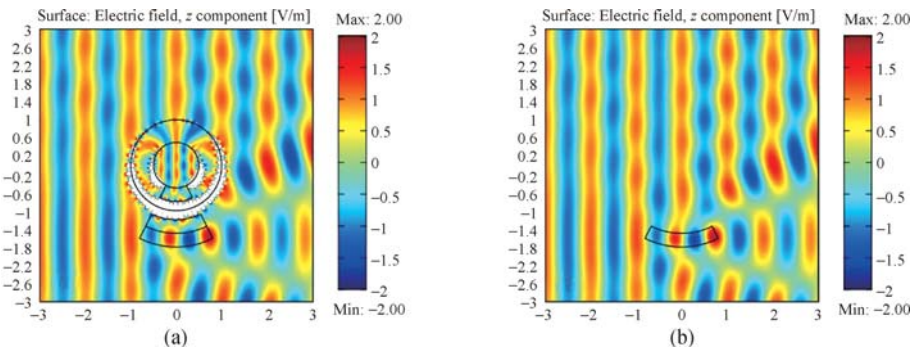


Fig. 4 Snapshots of the total electric fields under an incident TE plane wave from the left. (a) Demonstration of partial cloaking. The scattering pattern of a thick curved sheet with its inner parts “cloaked” by an illusion device is the same as that of a thin curved sheet, which is shown in (b).

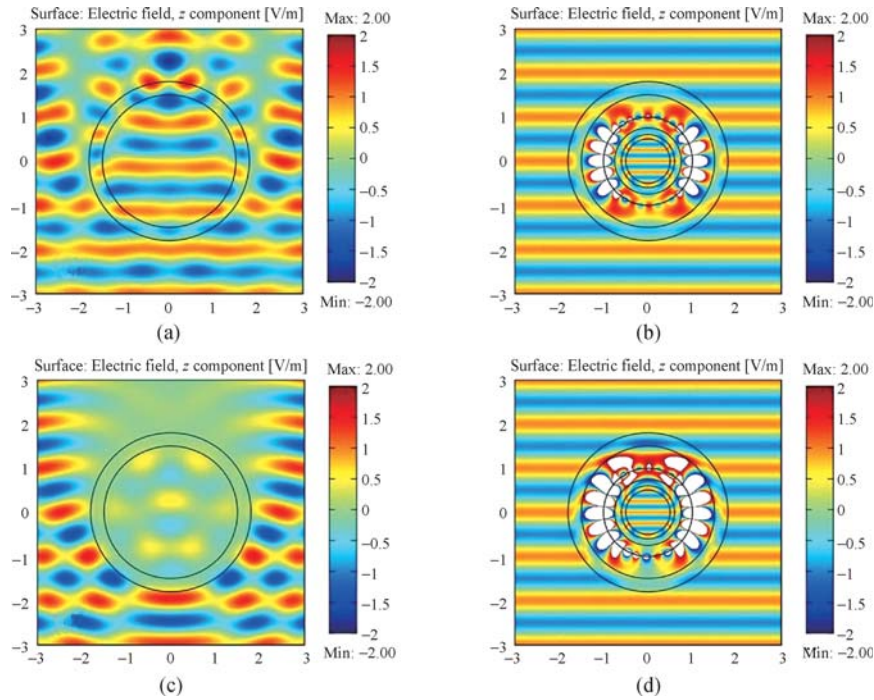


Fig. 5 Snapshots of the total electric fields under an incident TE plane wave from below. (a) A dielectric circular shell with permittivity $\epsilon_0 = 2$. (b) The circular shell in (a) is cloaked by an invisibility cloak placed within the shell. (c) A circular shell with permittivity $\epsilon_0 = -1$. (d) The circular shell in (c) is cloaked by a similar invisibility cloak as that in (b).

5(a), as well as its scattering pattern under a plane wave illumination from below. In this case, a complementary “image” shell with $\epsilon'_{oz} = 2\epsilon'_z$ and $\mu'_o = \mu'$, positioned between the circles of $r' = 0.6$ and $r' = 0.75$, is embedded inside the negative index complementary shell of the device shown in Fig. 3(a). In Fig. 5(b), we show that the dielectric shell are perfectly “cloaked” by an illusion device with embedded shell “image” from inside the shell instead of from outside, as the wave pattern is almost a perfect plane wave. In Fig. 5(c), we consider another circular shell of $\epsilon_0 = -1$ and $\mu_0 = 1$. The scattering pattern for such a shell, which is shown in Fig. 5(c), is similar to that of a metal shell. In this case, the complementary “image” shell with $\epsilon'_{oz} = -\epsilon'_z$ and $\mu'_o = \mu'$ is embedded. In Fig. 5(d), the calculated electric fields after the “metallic” shell is cloaked by the illusion de-

vice are shown. Again, an excellent cloaking effect is manifested by the perfect plane wave pattern.

3.4 Revealing a hidden object inside a container

Previously, we have shown that an object with a shell shape can be cloaked from inside. Here, we show that it can also be “removed” from outside such that a hidden object inside the shell can be revealed. As shown in Fig. 6(a), a dielectric object of $\epsilon = 5$ is hidden inside a circular opaque shell of $\epsilon = -1$. In Fig. 6(b), we show that when an illusion device is placed outside the opaque shell, light tunnels into interior domain and excite the hidden object. The scattering pattern outside the illusion device is almost the same as that of the hidden object itself, as shown in Fig. 6(c). Therefore, the

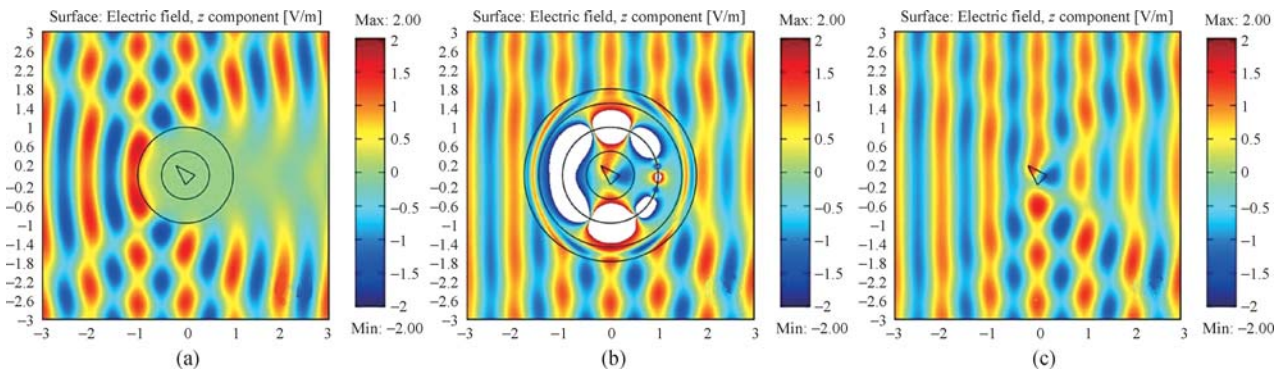


Fig. 6 Snapshots of the total electric fields under an incident TE plane wave from the left. (a) An object of $\epsilon = 5$ is hidden inside a circular opaque shell of $\epsilon = -1$. (b) An illusion device consisting of an inner shell of complementary medium and an outer shell of restoring medium is placed outside the opaque shell. It is clearly seen that the scattering pattern is changed into exactly the same pattern as the scattering pattern of the object itself, as shown in (c).

object is revealed by the illusion device. The illusion device consists of two shells, i.e., an inner shell of complementary medium “cancelling” the opaque shell ($1 < r' < 1.5$), and an outer shell of restoring medium that restores free space ($1.5 < r'' < 1.8$). The complementary medium layer is formed by the mapping $f(r') = 2 - r'$, while the restoring medium is formed by the mapping $f(r'') = 1.3(r'' - 1.8)/0.3 + 1.8$. By inserting the mappings into Eqs. (5) and (6), the parameters can be easily obtained.

4 Cloaking and illusion effects by using illusion devices designed in Cartesian geometry

4.1 Transforming the stereoscopic image of a dielectric spoon into that of a metallic cup

Previously, we have shown some cloaking effects of the illusion device designed in cylindrical geometry. In fact, the illusion device can be designed in any geometry. In the following, we demonstrate two applications of illusion devices designed in Cartesian geometry. The first one is an illusion device that transforms the stereoscopic image of a spoon of $\varepsilon_o = 2$ into that of a cup of $\varepsilon_i = -1$. Figure 7(a) and (c) plot, respectively, the scattering patterns of the dielectric spoon and the metallic cup, under the illumination of a TE plane wave of wavelength $\lambda = 0.25$ unit from below. In Fig. 7(b), an illusion device is placed beside the spoon. The scattering pattern around the spoon and the illusion device is altered in such a way that it appears as if there is only a metallic cup. This can be clearly seen by comparing the field patterns of the spoon plus the illusion device shown in Fig. 7(b) with that of the metallic cup shown in Fig. 7(c). The field patterns are indeed identical outside the virtual boundary. Inside the virtual boundary, the field patterns in Fig. 7(b) and (c) are completely different. Strong fields are localized on the surface of the illusion device due to the multiple scattering of light between the spoon and the illusion device. This indicates that the illusion effect is a steady-state

phenomenon that takes some time to establish.

The illusion device in Fig. 7(b) is composed of four parts of homogeneous media. The lower trapezoidal part is the “complementary medium” formed by a simple coordinate transformation of $y^{(2)} = -y^{(3)}/2$. It is composed of a negative index homogeneous medium of $\varepsilon_z^{(2)} = -2$, $\mu_x^{(2)} = -2$, and $\mu_y^{(2)} = -0.5$, with an embedded complementary “image” of the dielectric spoon with $\varepsilon_{oz}^{(2)} = -4$ and $\mu_o^{(2)} = \mu^{(2)}$. The upper left triangular part, the upper right triangular part, and the upper middle rectangular part collectively constitute the “restoring medium”. The upper left and right triangular parts are composed of a homogeneous medium with $\varepsilon_z^{(1)} = 4$, $\mu_{xx} = 4$, $\mu_{yy} = 20.5$, and $\mu_{xy} = \pm 9$, formed by the coordinate transformations of the forms $y^{(1)} \mp 3(x \pm 0.6) = 1/4 \cdot [y^{(4)} \mp 3(x \pm 0.6)]$, respectively. The upper middle rectangular part is composed of a homogeneous medium of $\varepsilon_z^{(1)} = 4$, $\mu_x^{(1)} = 4$, and $\mu_y^{(1)} = 0.25$, with an embedded compressed version of the metallic cup illusion of $\varepsilon_{iz}^{(1)} = -4$ and $\mu_i^{(1)} = \mu^{(1)}$, formed by the coordinate transformation of $y^{(1)} - 0.6 = 1/4 \cdot (y^{(4)} - 0.6)$. It is important to note that the homogeneity in the permittivity and permeability of the illusion device is a consequence of the simple Cartesian coordinate transformations applied here.

4.2 Seeing through a wall

Another interesting application of the illusion device in Cartesian geometry is that it enables people to open a virtual hole in a wall or obstacle. As shown before, the illusion device is capable of partial cloaking, i.e., transforming one part of an object into an illusion of free space, thus rendering that part invisible while leaving the rest of the object unaffected. By making one part of the wall invisible (i.e., making an illusion of a “hole”), we can see through the wall and obtain information from the other side. In Fig. 8(a), we see that a wall of $\varepsilon_o = -1$ with a width of 0.2 units is capable of blocking most of the energy of the TE electromagnetic waves of $\lambda = 0.25$ unit radiating from a Gaussian beam source

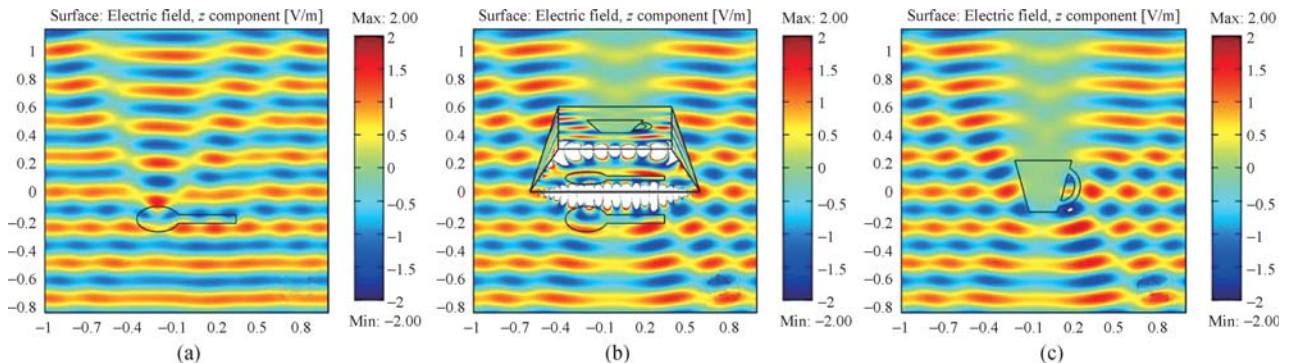


Fig. 7 Snapshots of the total electric fields under an incident TE plane wave from below. (a) The scattering pattern of the dielectric spoon. (b) The scattering pattern of the dielectric spoon is changed by the illusion device. Outside the virtual boundary, the scattering pattern becomes the same as that of the metallic cup, which is shown in (c).

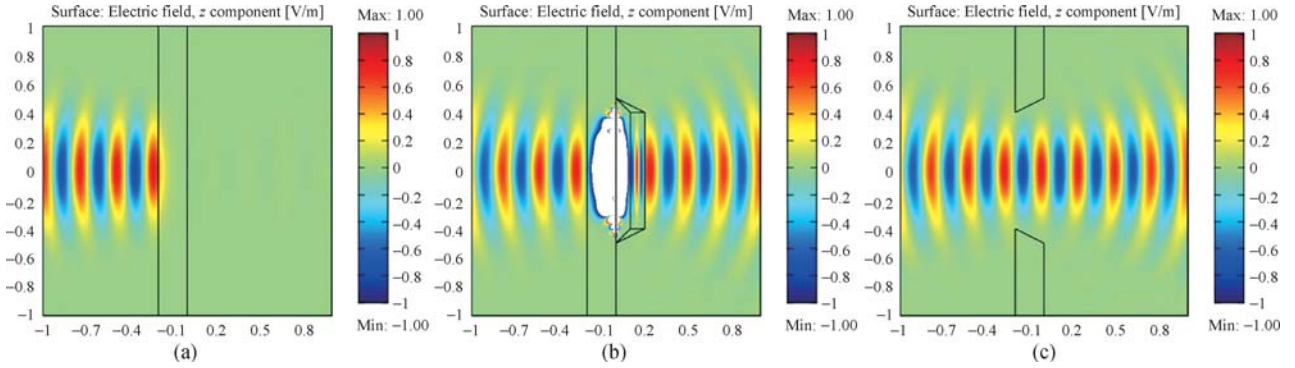


Fig. 8 Snapshots of the total electric fields under a TE Gaussian beam source incident from the left. (a) The radiation of the source is blocked by a slab of $\varepsilon_0 = -1$. (b) When an illusion device is attached to the wall, the electromagnetic radiation can now tunnel through the wall to the right side. The far field radiation pattern is exactly the same as that of the radiation through a real hole, which is shown in (c).

incident from the left. When the illusion device is placed on the right side of the wall, as shown in Fig. 8(b), the electromagnetic waves can penetrate through the wall as well as the illusion device and arrive on the right side. This effect can also be understood as the tunneling of electromagnetic waves via the high-intensity surface waves localized at the interface between the wall and the complementary medium. The phase information is accurately corrected by the restoring medium in the illusion device, such that the transmitted field patterns on the right side become the same as those of the electromagnetic waves penetrating through a real hole, as shown in Fig. 8(c). Thus, an observer on the right side can peep through the virtual hole as if he/she is peeping through a real hole at the working frequency of the illusion device.

The illusion device in Fig. 8(b) is also composed of four parts. The left trapezoidal part in contact with the wall is the complementary medium with $\varepsilon_z^{(2)} = 2$, $\mu_{xx}^{(2)} = -0.5$, and $\mu_{yy}^{(2)} = -2$, formed by a coordinate transformation of $x^{(2)} = -x^{(3)}/2$. Here, the complementary medium is only negative in permeability because the “cancelled” wall is negative in permittivity (i.e., metallic). The upper and lower triangular parts and the middle rectangular part on the right constitute the restoring medium. The upper and lower triangular parts are composed of a medium with $\varepsilon_z^{(1)} = 4$, $\mu_{xx}^{(1)} = 9.25$, $\mu_{yy}^{(1)} = 4$, and $\mu_{xy}^{(1)} = \mp 6$, formed by the coordinate transformations of the forms $x^{(1)} \pm 2(y \mp 0.5) = 1/4 \cdot [x^{(4)} \pm 2(y \mp 0.5)]$, respectively. The middle rectangular part is composed of a medium of $\varepsilon_z^{(1)} = 4$, $\mu_x^{(1)} = 0.25$, and $\mu_y^{(1)} = 4$, formed by the coordinate transformation of $x^{(1)} - 0.2 = 1/4 \cdot (x^{(4)} - 0.2)$. This “peeping” device does not require a broad bandwidth and thus can be constructed by resonant metamaterials designed at a single selected working frequency.

5 Conclusions and discussion

We have reviewed the principle of an illusion device that

is capable of transforming the stereoscopic image of an object into that of an illusion of our choice. When the illusion is that of free space, cloaking is realized. Unlike previous light-bending cloaks, this illusion device is based on a “cancel and restore” scheme. First, the object is optically “cancelled” by a complementary medium embedded with a complementary “image” of the object. Then, a stereoscopic illusion is created by a restoring medium that “restores” the “cancelled” space. Due to its unique principle, this illusion device can have various novel applications. Some of them have been shown in this review.

Finally, we would like to discuss a bit about the feasibility of realizing this illusion device. Currently, the biggest difficulty to realize illusion optics may lie in the fabrication of metamaterials, especially negative index materials. In the numerical simulations shown above, we find that there are usually strong and fast oscillating surface waves on the surface of negative index materials, especially when the virtual boundary of the illusion device has a large range. This indicates that the negative index materials must not have large absorption as well as defects, as both of them could have compromised or deformed the surface waves dramatically. For instance, we find that when a tiny absorption of certain order is put in the negative permittivity of the complementary medium, the cloaking or illusion effect could be compromised. Since we have used very dense meshes in the finite element simulation, especially near the surface of the complementary medium, the lattice constant of the metamaterial also have a strong requirement as it must be smaller than the mesh size such that the effective medium description of the metamaterial is still applicable. However, these issues are mostly technical ones. As the fabrication technique of metamaterials is improving fast, we expect that sufficiently fine and low-loss negative index materials would be created eventually, and then, the realization of remote illusion optics will not be far away.

Acknowledgements This work was supported by Hong Kong RGC Grant No. 600209. Computation resources were supported by Shun Hing Education and Charity Fund. We thank Drs. D. Z. Han, J. J. Xiao, K. H. Fung, Z. H. Hang, Jeffrey C. W. Lee and H. H. Zheng for helpful discussions.

References

1. U. Leonhardt, *Science*, 2006, 312: 1777
2. J. B. Pendry, D. Schurig, and D. R. Smith, *Science*, 2006, 312: 1780
3. A. Greenleaf, M. Lassas, and G. Uhlmann, *Physiol. Meas.*, 2003, 24: 413
4. G. W. Milton, M. Briane, and J. R. Willis, *New J. Phys.*, 2006, 8: 248
5. U. Leonhardt and T. G. Philbin, *New J. Phys.*, 2006, 8: 247
6. S. A. Cummer, B. I. Popa, D. Schurig, D. R. Smith, and J. B. Pendry, *Phys. Rev. E*, 2006, 74: 036621
7. H. Y. Chen, Z. X. Liang, P. J. Yao, X. Y. Jiang, H. R. Ma, and C. T. Chan, *Phys. Rev. B*, 2007, 76: 241104
8. Z. Ruan, M. Yan, C. W. Neff, and M. Qiu, *Phys. Rev. Lett.*, 2007, 99: 113903
9. H. Chen, B. I. Wu, B. Zhang, and J. A. Kong, *Phys. Rev. Lett.*, 2007, 99: 063903
10. M. Rahm, D. Schurig, D. A. Roberts, S. A. Cummer, D. R. Smith, and J. B. Pendry, *Photon. Nanostruct: Fundam. Applic.*, 2008, 6: 87
11. A. V. Kildishev, W. Cai, U. K. Chettiar, and V. M. Shalaev, *New J. Phys.*, 2008, 10: 115029
12. D. Schurig, J. J. Mock, B. J. Justice, S. A. Cummer, J. B. Pendry, A. F. Starr, and D. R. Smith, *Science*, 2006, 314: 977
13. W. Cai, U. K. Chettiar, A. V. Kildishev, and V. M. Shalaev, *Nature Photonics*, 2007, 1: 224
14. U. Leonhardt and T. Tyc, *Science*, 2009, 323: 110
15. J. Li and J. B. Pendry, *Phys. Rev. Lett.*, 2008, 101: 203901
16. R. Liu, C. Ji, J. J. Mock, J. Y. Chin, T. J. Cui, and D. R. Smith, *Science*, 2009, 323: 366
17. L. H. Gabrielli, J. Cardenas, C. B. Poitras, and M. Lipson, *Nature Photonics*, 2009, 3: 461
18. J. Valentine, J. Li, T. Zentgraf, G. Bartal, and X. Zhang, *Nature Materials*, 2009, 8: 568
19. I. I. Smolyaninov, V. N. Smolyaninova, A. V. Kildishev, and V. M. Shalaev, *Phys. Rev. Lett.*, 2009, 102: 213901
20. A. Alu and N. Engheta, *Phys. Rev. E*, 2005, 72: 016623
21. A. Alu and N. Engheta, *Phys. Rev. Lett.*, 2008, 100: 113901
22. A. Alu and N. Engheta, *Phys. Rev. Lett.*, 2009, 102: 233903
23. G. A. Zheng, X. Heng, and C. H. Yang, *New J. Phys.*, 2009, 11: 033010
24. J. M. Hao, W. Yan, and M. Qiu, arXiv: 0906.5543, 2009
25. G. W. Milton and N. A. P. Nicorovici, *Proc. R. Soc. A*, 2006, 462: 3027
26. N. A. P. Nicorovici, G. W. Milton, R. C. McPhedran, and L. C. Botten, *Opt. Express*, 2007, 15: 6314
27. O. P. Bruno and S. Lintner, *J. Appl. Phys.*, 2007, 102: 124502
28. Y. Lai, H. Y. Chen, Z. Q. Zhang, and C. T. Chan, *Phys. Rev. Lett.*, 2009, 102: 093901
29. D. A. B. Miller, *Opt. Express*, 2006, 14: 12457
30. F. G. Vasquez, G. W. Milton, and D. Onofrei, *Phys. Rev. Lett.*, 2009, 103: 073901
31. F. G. Vasquez, G. W. Milton, and D. Onofrei, *Opt. Express*, 2009, 17: 14800
32. H. H. Zheng, J. J. Xiao, Y. Lai, and C. T. Chan, arXiv: 0908.2279, 2009
33. Y. Lai, J. Ng, H. Y. Chen, D. Z. Han, J. J. Xiao, Z. Q. Zhang, and C. T. Chan, *Phys. Rev. Lett.*, 2009, 102: 253902
34. M. Yan, W. Yan, and M. Qiu, *Phys. Rev. B*, 2008, 78: 125113
35. Y. Luo, J. J. Zhang, H. Chen, B. I. Wu, and J. A. Kong, arXiv: 0818.0215, 2008
36. T. Yang, H. Y. Chen, X. D. Luo, and H. R. Ma, *Opt. Express*, 2008, 16: 18545
37. X. D. Luo, Y. Tao, Y. W. Gu, H. Y. Chen, and H. R. Ma, *Appl. Phys. Lett.*, 2009, 94: 223513
38. H. Y. Chen, X. H. Zhang, X. D. Luo, H. R. Ma, and C. T. Chan, *New J. Phys.*, 2008, 10: 113016
39. J. Ng, H. Y. Chen, and C. T. Chan, *Opt. Lett.*, 2009, 34: 644
40. H. Y. Chen, C. T. Chan, S. Y. Liu, and Z. F. Lin, *New J. Phys.*, 2009, 11: 083012
41. W. X. Jiang, H. F. Ma, Q. Cheng, and T. J. Cui, arXiv: 0909.3619, 2009
42. W. X. Jiang and T. J. Cui, arXiv: 0909.5255, 2009
43. H. Y. Chen and C. T. Chan, *Appl. Phys. Lett.*, 2007, 90: 241105
44. A. V. Kildishev and E. E. Narimanov, *Opt. Lett.*, 2007, 32: 3432
45. H. Y. Chen, X. D. Luo, H. R. Ma, and C. T. Chan, *Opt. Express*, 2008, 16: 14603
46. M. Rahm, S. A. Cummer, D. Schurig, J. B. Pendry, and D. R. Smith, *Phys. Rev. Lett.*, 2008, 100: 063903
47. H. Y. Chen and C. T. Chan, *Phys. Rev. B*, 2008, 78: 054204
48. J. J. Zhang, Y. Luo, H. S. Chen, J. T. Huangfu, B. I. Wu, L. X. Ran, and J. A. Kong, *Opt. Express*, 2009, 17: 6203
49. A. Greenleaf, Y. Kurylev, M. Lassas, and G. Uhlmann, *Phys. Rev. Lett.*, 2007, 99: 183901
50. D. A. Genov, S. Zhang, and X. Zhang, *Nature Physics*, 2009, 5: 687
51. J. B. Pendry, A. J. Holden, D. J. Robbins, and W. J. Stewart, *IEEE Trans. Microwave Theory Tech.*, 1999, 47: 2075
52. D. R. Smith, J. B. Pendry, and M. C. K. Wiltshire, *Science*, 2004, 305: 788
53. C. M. Soukoulis, S. Linden, and M. Wegener, *Science*, 2007, 315: 47
54. H. J. Lezec, J. A. Dionne, and H. A. Atwater, *Science*, 2007, 316: 430
55. J. Valentine, S. Zhang, T. Zentgraf, E. Ulin-Avila, D. A.

- Genov, G. Bartal, and X. Zhang, *Nature*, 2008, 455: 376
56. J. Yao, Z. W. Liu, Y. M. Liu, Y. Wang, C. Sun, G. Bartal, A. M. Stacy, and X. Zhang, *Science*, 2008, 321: 930
57. J. B. Pendry, *Phys. Rev. Lett.*, 2000, 85: 3966
58. J. B. Pendry and S. A. Ramakrishna, *J. Phys.: Condens. Matter*, 2002, 14: 8463
59. J. B. Pendry and S. A. Ramakrishna, *J. Phys.: Condens. Matter*, 2003, 15: 6345